

Magnetohydrodynamic convective flow in a rotating channel

S. K. GHOSH ⁽¹⁾ and P. K. BHATTACHARJEE ⁽²⁾

⁽¹⁾ *Department of Mathematics Narajole Raj College
P.O.: Narajole, Dist: Midnapore West Bengal, India*

⁽²⁾ *Department of Applied Mathematics Vidyasagar University
Midnapore West Bengal, India*

COMBINED FREE AND FORCED convective flow of an electrically conducting viscous incompressible fluid in a rotating parallel plate channel with perfectly conducting walls is investigated. Exact solutions of the governing equations for the fully developed flow are obtained in closed form. It is found that the resultant shear stresses at the walls decrease with the increase in both the rotation parameter K^2 and the magnetic parameter M^2 . The rate of heat transfer at both walls decreases with the increase in the Grashof number G .

1. Introduction

THE STUDY OF FLUID FLOWS subject to the magnetic field and rotation finds wide applications in many fields of geophysical and astrophysical interest. VIDYANIDHI [1] has considered the effect of rotation on the hydromagnetic flow within a non-conducting parallel plate channel. On the other hand, NANDA and MOHANTY [2] have investigated the hydromagnetic flow in a rotating channel with perfectly conducting walls. However, the effect of combined free and forced convection flow does not receive much attention in literature. However, this study may have some bearings on the process of cooling of turbine blades, power generation, geophysical and astrophysical problems. Recently GUPTA [3] has studied the effect of combined free and forced convection on the flow of a viscous incompressible fluid in a parallel plate channel rotating with uniform angular velocity about an axis perpendicular to the plates.

In the present paper we have considered the combined free and forced convective flow of an electrically conducting viscous incompressible fluid confined between two horizontal perfectly conducting plates, rotating at a uniform angular velocity Ω about an axis perpendicular to their planes, in the presence of an applied uniform transverse magnetic field parallel to the axis of rotation. Exact solution of the governing equations for the fully developed flow is obtained in a closed form. The asymptotic behaviour of the solution is also analysed for both

small and large rotation parameter K^2 and the magnetic parameter M^2 , to get some physical insight into the flow pattern. Heat transfer characteristics are also studied taking into account the viscous and Joule dissipations.

2. Mathematical formulation and its solution

Consider the steady, fully developed combined free and forced convection flow of an electrically conducting viscous incompressible fluid within a perfectly conducting parallel plate channel $z = \pm L$ due to a constant pressure gradient along the x -axis. A uniform magnetic flux density B_0 is imposed along the z -axis about which both the fluid and plates rotate at a uniform angular velocity Ω .

Since the plates of the channel are infinite in the x and y directions, all physical quantities except the pressure and temperature will be functions of z only. Rotation induces cross-flow, the velocity of fluid and magnetic field may be assumed as $q = (u^*, v^*, 0)$ and $B = (B_x^*, B_y^*, B_0)$, respectively, compatible with the fundamental equations of magnetohydrodynamics where \mathbf{q} is the velocity vector and \mathbf{B} is the magnetic field vector. The equation of continuity leads to a conservation of mass i.e. $\nabla \cdot q = 0$ and the solenoidal relation is $\nabla \cdot B = 0$. Therefore, under these assumptions, the equations of momentum and the magnetic induction in a rotating frame of reference can be written as

$$(2.1) \quad -2\rho\Omega v^* = -\frac{\partial P}{\partial x} + \mu \frac{\partial^2 u^*}{\partial z^2} + \frac{B_0}{\mu_e} \frac{\partial B_x^*}{\partial z},$$

$$(2.2) \quad 2\rho\Omega u^* = \mu \frac{\partial^2 v^*}{\partial z^2} + \frac{B_0}{\mu_e} \frac{\partial B_y^*}{\partial z},$$

$$(2.3) \quad 0 = -\frac{\partial p}{\partial z} - \rho g - \frac{1}{\mu_e} \left(B_x^* \frac{\partial B_x^*}{\partial z} + B_y^* \frac{\partial B_y^*}{\partial z} \right),$$

$$(2.4) \quad \frac{\partial^2 B_x^*}{\partial z^2} + \sigma \mu_e B_0 \frac{\partial u^*}{\partial z} = 0,$$

$$(2.5) \quad \frac{\partial^2 B_y^*}{\partial z^2} + \sigma \mu_e B_0 \frac{\partial v^*}{\partial z} = 0,$$

where ρ , μ , μ_e , σ , g and p are, respectively, the fluid density, coefficient of viscosity, magnetic permeability, electrical conductivity, acceleration due to gravity and modified pressure including the centrifugal force.

Assuming uniform axial temperature variation along the channel walls, the temperature of the fluid can be assumed in the form

$$(2.6) \quad T - T_0 = Nx + \phi(z),$$

where N is the uniform temperature gradient, T is the fluid temperature and T_0 is the temperature in the reference state.

Using the equation of state under the Boussinesq approximation

$$(2.7) \quad \rho = \rho_0[1 - \beta(T - T_0)].$$

We obtain from Eq. (2.3) after integration

$$(2.8) \quad p = -\rho_0 g \int [1 - \beta(T - T_0)] dz - \frac{1}{2\mu_e} (B_x^{*2} + B_y^{*2}) + F^*(x),$$

where β is the coefficient of thermal expansion and ρ_0 is the density of reference state.

Making use of Eqs. (2.6) and (2.8) in Eq. (2.1), we obtain

$$(2.9) \quad -2\Omega v^* = -g\beta Nz - \frac{1}{\rho_0} \frac{dF^*(x)}{dx} + \nu \frac{d^2 u^*}{dz^2} + \frac{B_0}{\mu_e \rho_0} \frac{dB_x^*}{dz},$$

where $\nu = \mu/\rho_0$.

Introducing non-dimensional variables

$$(2.10) \quad \eta = \frac{z}{L}, \quad u = \frac{u^* L}{\nu R}, \quad v = \frac{v^* L}{\nu R},$$

$$B_x = B_x^*/\sigma\mu_e\nu B_0 R, \quad B_y = B_y^*/\sigma\mu_e\nu B_0 R, \quad R = (L^3/\rho_0\nu^2) \left(-\frac{dF^*}{dx}\right),$$

Equations (2.9), (2.2), (2.4) and (2.5) reduce to

$$(2.11) \quad \frac{d^2 u}{d\eta^2} + M^2 \frac{dB_x}{d\eta} + 2K^2 v = -1 + G\eta,$$

$$(2.12) \quad \frac{d^2 v}{d\eta^2} + M^2 \frac{dB_y}{d\eta} - 2K^2 u = 0,$$

$$(2.13) \quad \frac{d^2 B_x}{d\eta^2} + \frac{du}{d\eta} = 0,$$

$$(2.14) \quad \frac{d^2 B_y}{d\eta^2} + \frac{dv}{d\eta} = 0,$$

where $M = B_0 L(\sigma/\rho_0\nu)^{1/2}$ is the Hartmann number, $K^2 = \Omega L^2/\nu$ is the rotation parameter, and $G = g\beta N L^4/\nu^2 R$ is the Grashof number.

The boundary conditions for the velocity field are the usual no-slip conditions at the plates, i.e.

$$(2.15) \quad u = v = 0 \quad \text{at } \eta = \pm 1.$$

Since the plates are assumed to be perfectly conducting, the boundary conditions for magnetic field are

$$(2.16) \quad \frac{dB_x}{d\eta} = \frac{dB_y}{d\eta} = 0 \quad \text{at } \eta = \pm 1.$$

Combining Eqs. (2.11) and (2.13) with Eqs. (2.12) and (2.14) respectively, we obtain

$$(2.17) \quad \frac{d^2 F}{d\eta^2} + M^2 \frac{db}{d\eta} - 2iK^2 F = -1 + G\eta,$$

$$(2.18) \quad \frac{d^2 b}{d\eta^2} + \frac{dF}{d\eta} = 0,$$

where

$$(2.19) \quad F = u + iv \quad \text{and } b = B_x + iB_y.$$

The boundary conditions (2.15) and (2.16) become

$$(2.20) \quad F = 0 \quad \text{and } \frac{db}{d\eta} = 0 \quad \text{at } \eta = \pm 1.$$

The solution of Eqs. (2.17) and (2.18) subject to the boundary conditions (2.20) is

$$(2.21) \quad F(\eta) = \frac{(\alpha - i\beta)^2}{(\alpha^2 + \beta^2)^2} \left[\left(1 - \frac{\text{ch}(\alpha + i\beta)\eta}{\text{ch}(\alpha + i\beta)} \right) + G \left(\frac{\text{sh}(\alpha + i\beta)\eta}{\text{sh}(\alpha + i\beta)} - \eta \right) \right],$$

$$(2.22) \quad b(\eta) = \frac{(\alpha - i\beta)^2}{(\alpha^2 + \beta^2)^2} \left[\left(\frac{\text{sh}(\alpha + i\beta)\eta}{(\alpha + i\beta)\text{ch}(\alpha + i\beta)} - \eta \right) + \frac{G}{2} \left(\eta^2 - \frac{2\text{ch}(\alpha + i\beta)\eta}{(\alpha + i\beta)\text{sh}(\alpha + i\beta)} + \frac{2\text{cth}(\alpha + i\beta)}{(\alpha + i\beta)} - 1 \right) \right],$$

where

$$(2.23) \quad \alpha = \frac{1}{\sqrt{2}} \left[(M^4 + 4K^4)^{1/2} + M^2 \right]^{1/2},$$

$$\beta = \frac{1}{\sqrt{2}} \left[(M^4 + 4K^4)^{1/2} - M^2 \right]^{1/2}.$$

Considering the expressions of $F(\eta)$ and $b(\eta)$ given by (2.19), one can easily obtain the x and y components of the velocity and magnetic field from Eqs. (2.21) and (2.22), respectively.

In the absence of the buoyancy force (i.e. $G = 0$), the solutions (2.21) and (2.22) reduce to the results obtained by NANDA and MOHANTY [2].

Now we shall discuss a few particular cases of interest of the general solution given by Eqs. (2.21) and (2.22).

Case 1: $M^2 \ll 1$ and $K^2 \ll 1$

Since M^2 and K^2 are very small, neglecting higher powers of M^2 and K^2 in Eqs. (2.21) and (2.22), we obtain

$$(2.24) \quad u = \frac{1}{2}(1 - \eta^2) + \frac{1}{3}G(\eta^3 - \eta) + M^2 \left[-\frac{1}{24}(5 - 6\eta^2 + \eta^4) + \frac{G}{360}(7\eta - 10\eta^3 + 3\eta^5) \right] + \dots,$$

$$(2.25) \quad v = K^2 \left[-\frac{1}{12}(5 - 6\eta^2 + \eta^4) + \frac{G}{180}(7\eta - 10\eta^3 + 3\eta^5) \right] + \dots,$$

$$(2.26) \quad B_x = \frac{1}{6}(\eta^3 - \eta) + \frac{G}{24}(-1 + 2\eta^2 - \eta^4) + M^2 \left[\frac{1}{24} \left(5\eta - 2\eta^3 - \frac{1}{5}\eta^5 \right) + \frac{G}{720}(7\eta^2 - 5\eta^4 + \eta^6) \right] + \dots,$$

$$(2.27) \quad B_y = K^2 \left[\frac{1}{12} \left(5\eta - 2\eta^3 + \frac{1}{5}\eta^5 \right) - \frac{G}{360}(7\eta^2 - 5\eta^4 + \eta^6) \right] + \dots$$

Equations (2.24) – (2.27) reveal that in a slowly rotating system when the conductivity of fluid is low and the applied magnetic field is weak, the effect of magnetic field on the secondary flow v and on the induced magnetic field component B_y is negligible while the primary flow u and the induced magnetic field component B_x are unaffected by rotation. In absence of the rotation and magnetic fields, the problem reduces to the free and forced convection flow through a horizontal parallel plate channel due to a constant pressure gradient. In this case, the critical Grashof number $G_{\text{crit}} = \frac{1}{2}$.

Case 2: $K^2 \gg 1$ and $M^2 \sim O(1)$.

When rotation is very large and the applied magnetic field is weak, we can expect a boundary layer type of flow. For the boundary layer on the upper plate $\eta = 1$, writing $(1 - \eta) = \xi$, we obtain from Eqs. (2.21) and (2.22) the results

$$(2.28) \quad u = \frac{(1-G)}{2K^2} \exp \left[-K \left(1 + \frac{M^2}{4K^2} \right) \xi \right] \sin \left[K \left(1 - \frac{M^2}{4K^2} \right) \xi \right],$$

$$(2.29) \quad v = \frac{1}{2K^2} \left[-1 + (1-\xi)G + (1-G) \exp \left\{ -K \left(1 + \frac{M^2}{4K^2} \right) \xi \right\} \right. \\ \left. \times \cos \left\{ K \left(1 - \frac{M^2}{4K^2} \right) \xi \right\} \right],$$

$$(2.30) \quad B_x = -\frac{1}{2K^3} \left[\frac{1}{2}G + \frac{(1-G)}{\sqrt{2}} \exp \left\{ -K \left(1 + \frac{M^2}{4K^2} \right) \xi \right\} \right. \\ \left. \times \sin \left\{ K \left(1 - \frac{M^2}{4K^2} \right) \xi + \frac{\pi}{4} \right\} \right],$$

$$(2.31) \quad B_y = -\frac{1}{2K^3} \left[K \left\{ -1 + \xi + \frac{1}{2}G\xi(\xi-2) \right\} + \frac{G}{2} + \frac{(1-G)}{\sqrt{2}} \right. \\ \left. \times \exp \left\{ -K \left(1 + \frac{M^2}{4K^2} \right) \xi \right\} \cos \left\{ K \left(1 - \frac{M^2}{4K^2} \right) \xi + \frac{\pi}{4} \right\} \right].$$

Equations (2.28) – (2.31) demonstrate the existence of a thin boundary layer of thickness $O \left\{ K \left(1 + \frac{M^2}{4K^2} \right) \right\}^{-1}$ in the vicinity of the wall ($\eta = 1$). This layer may be identified as a hydromagnetic Ekman layer and can be considered as a classical Ekman boundary layer modified by a uniform applied magnetic field parallel to the axis of rotation. The exponential terms in the expressions (2.28) – (2.31) damp out quickly as ξ increases. When $\xi \geq \frac{1}{K(1 + M^2/4K^2)}$, we have

$$(2.32) \quad u \approx 0, \quad v \approx \frac{1}{2K^2} [-1 + (1-\xi)G],$$

$$(2.33) \quad B_x \approx -\frac{G}{4K^3}, \quad B_y \approx -\frac{1}{2K^3} \left[K \left\{ -1 + \xi + \frac{1}{2}G\xi(\xi-2) \right\} + \frac{G}{2} \right].$$

Equation (2.32) reveals that in the certain core, given by $\xi \geq 1/K(1 + M^2/4K^2)$ about the axis of the channel, i.e. outside the boundary layer region, the velocity in the direction of pressure gradient vanishes while it remains in the y -direction. Thus, in the central core, the fluid will be moving in a direction normal to the pressure gradient and the axis of rotation. It is also evident from Eqs. (2.32) and (2.33) that, in the central core, the velocity and the magnetic field components

are independent of the applied magnetic field, and the magnetic field component B_x is very weak of order $O(G/4K^2)$.

Case 3: $M^2 \gg 1$ and $K^2 \sim O(1)$.

In this case also the flow has a boundary layer character and we obtain the velocity and magnetic field components from Eqs. (2.21) and (2.22) as

$$(2.34) \quad u = \frac{1}{M^2} [(1 - \exp(-M\xi)) + G \{-1 + \xi + \exp(-M\xi)\}],$$

$$(2.35) \quad v = \frac{K^2}{M^4} [\{(2 + M\xi) \exp(-M\xi) - 2\} + G \{2(1 - \xi) - (2 + M\xi) \exp(-M\xi)\}],$$

$$(2.36) \quad B_x = \frac{1}{M^2} \left[\left\{ -1 + \xi + \frac{1}{M} \exp(-M\xi) \right\} + G \left\{ \frac{1}{2} \xi (2 - \xi) + \frac{1}{M} (1 - \exp(-M\xi)) \right\} \right],$$

$$(2.37) \quad B_y = \frac{K^2}{M^4} \left[\left\{ 2 - (2 + \frac{1}{M} \exp(-M\xi)) \xi - \frac{3}{M} \exp(-M\xi) + G \{ \xi (2 - \xi) - \frac{1}{M} (3 - \xi M \exp(-M\xi)) + \frac{3}{M} \exp(-M\xi) \} \right\} \right].$$

Expressions (2.34) – (2.37) demonstrate the existence of a thin boundary layer of thickness $O(1/M)$ near the plate $\eta = 1$ which is independent of the rotation parameter K^2 . This layer may be identified as the Hartmann layer. It is interesting to note that the secondary velocity v and magnetic field B_y are very weak being $O(K^2/M^4)$, while the primary velocity u and magnetic field B_x are unaffected by the rotation of the fluid. Therefore from expressions (2.34) and (2.35) we may conclude that in the central core given by $\xi \geq \frac{1}{4}$ the fluid will be moving in the direction of the pressure gradient.

3. Results and discussion

The non-dimensional shear stress components at the plates $\eta = \pm 1$ are

$$(3.1) \quad \left. \frac{du}{d\eta} \right|_{\eta=\pm 1} = \frac{1}{(\alpha^2 + \beta^2)} \left[\mp \frac{\alpha \operatorname{sh} 2\alpha + \beta \sin 2\beta}{(\operatorname{ch} 2\alpha + \cos 2\beta)} + G \left\{ \frac{\alpha \operatorname{sh} 2\alpha - \beta \sin 2\beta}{(\operatorname{ch} 2\alpha - \cos 2\beta)} - \frac{(\alpha^2 - \beta^2)}{(\alpha^2 + \beta^2)} \right\} \right],$$

$$(3.2) \quad \left. \frac{dv}{d\eta} \right|_{\eta=\pm 1} = -\frac{1}{(\alpha^2 + \beta^2)} \left[\mp \frac{\beta \operatorname{sh} 2\alpha - \alpha \sin 2\beta}{(\operatorname{ch} 2\alpha + \cos 2\beta)} + G \left\{ \frac{\beta \operatorname{sh} 2\alpha + \alpha \sin 2\beta}{(\operatorname{ch} 2\alpha - \cos 2\beta)} - \frac{2\alpha\beta}{(\alpha^2 + \beta^2)} \right\} \right].$$

The upper and lower signs in the Eqs. (3.1) and (3.2) correspond to values at the upper wall ($\eta = +1$) and the lower wall ($\eta = -1$), respectively.

The primary shear stress $\left. \frac{du}{d\eta} \right|_{\eta=-1}$ will vanish if the critical Grashof number equals

$$(3.3) \quad G_{cx} = -\frac{a_1(\alpha \operatorname{sh} 2\alpha + \beta \sin 2\beta)}{(a_2 - a_3)},$$

where

$$(3.4) \quad \begin{aligned} a &= \operatorname{ch} 2\alpha - \cos 2\beta, \\ a_1 &= a(\alpha^2 + \beta^2)/(\sigma \operatorname{ch} 2\alpha + \cos 2\beta), \\ a_2 &= (\alpha^2 + \beta^2)\alpha \operatorname{sh} 2\alpha + a\beta^2, \\ a_3 &= (\alpha^2 + \beta^2)\beta \sin 2\beta + a\alpha^2. \end{aligned}$$

The numerator in (3.3) is always positive, since $\operatorname{ch} 2\alpha > \cos 2\beta$ for all values of M^2 and K^2 . Thus when $a_2 > a_3$, there will be an incipient primary flow reversal at the lower plate when the temperature of the lower plate decreases.

Similarly, the secondary shear stress $\left. \frac{dv}{d\eta} \right|_{\eta=-1}$ will vanish if the critical Grashof number equals

$$(3.5) \quad G_{cy} = -\frac{a_1(\beta \operatorname{sh} 2\alpha - \alpha \sin 2\beta)}{(a_4 - a_5)},$$

where

$$(3.6) \quad \begin{aligned} a_4 &= (\alpha^2 + \beta^2)(\beta \operatorname{sh} 2\alpha + \alpha \sin 2\beta), \\ a_5 &= (2\alpha\beta)(\operatorname{ch} 2\alpha - \cos 2\beta). \end{aligned}$$

Equations (3.5) and (3.6) show that for the decrease in the temperature at the lower wall, there will be an incipient reversed secondary flow near the lower wall ($\eta = -1$), $\beta \text{sh}2\alpha > \alpha \sin 2\beta$ and $a_4 > a_5$ or $\beta \text{sh}2\alpha < \alpha \sin 2\beta$ and $a_4 < a_5$. Also due to the increase in temperature in the axial direction of the lower plate, the secondary flow shows the reversal when $\beta \text{sh}2\alpha > \alpha \sin 2\beta$ and $a_4 > a_5$ or $\beta \text{sh}2\alpha < \alpha \sin 2\beta$ and $a_4 < a_5$. Proceeding exactly in the same way, we observe that the primary flow reversal near the upper plate $\eta = 1$ occurs, if

$$(3.7) \quad G_{cx} = \frac{a_1(\alpha \text{sh}2\alpha + \beta \sin 2\beta)}{(a_2 - a_3)}.$$

Equation (3.7) reveals that the primary flow reversal occurs only when temperature of the upper wall increases in the axial direction.

Similarly, for secondary flow reversal at the upper plate $\eta = 1$, we get

$$(3.8) \quad G_{cy} = \frac{a_1(\beta \text{sh}2\alpha - \alpha \sin 2\beta)}{(a_4 - a_5)}.$$

Equations (3.7) and (3.8) are the same as (3.3) and (3.5) respectively, taken with opposite sign.

The values of the critical Grashof numbers G_{cx} and G_{cy} given by (3.3) and (3.5), respectively, for which the primary and secondary flow reversal occur near the lower plate, are given in Tables 1 and 2 for various values of K^2 and M^2 . It is observed that G_{cx} and G_{cy} decrease with the increase in the rotation parameter K^2 . Hence we may conclude that rotation exerts a destabilizing effect on the primary as well as on the secondary flow.

Table 1. Critical Grashof number G_{cx} .

M^2/K^2	1.0	2.0	3.0	25.0	81.0
10	1.437079	1.403206	1.356935	1.036904	1.006681
15	1.340707	1.327579	1.307924	1.052206	1.009877
20	1.285041	1.278675	1.268736	1.065118	1.012967
25	1.248529	1.244960	1.239268	1.075641	1.015942

Table 2. Critical Grashof number G_{cy} .

M^2/K^2	1.0	2.0	3.0	25.0	81.0
10	2.439813	2.351326	2.229098	1.276532	1.129143
15	2.009786	1.979156	1.933043	1.285473	1.131058
20	1.791160	1.777421	1.755917	1.291425	1.132857
25	1.659765	1.652515	1.640924	1.294541	1.134537

The resultant shear stresses at the plates $\eta = 1$ and $\eta = -1$ are, respectively,

$$(3.9) \quad \tau_1 = \left\{ \left(\frac{du}{d\eta} \right)_{\eta=1}^2 + \left(\frac{dv}{d\eta} \right)_{\eta=1}^2 \right\}^{1/2},$$

and

$$(3.10) \quad \tau_2 = \left\{ \left(\frac{du}{d\eta} \right)_{\eta=-1}^2 + \left(\frac{dv}{d\eta} \right)_{\eta=-1}^2 \right\}^{1/2}.$$

The values of τ_1 and τ_2 have been calculated numerically and are presented in Tables 3 and 4 for various values of K^2 and M^2 . It is observed that both τ_1 and τ_2 decrease with the increase in either K^2 or M^2 .

Table 3. Resultant shear stress τ_1 at the plate $\eta = 1$ for $G = 0.2$.

M^2/K^2	1.0	2.0	3.0	25.0	81.0
10	0.268977	0.261635	0.251059	0.115098	0.063697
15	0.218611	0.215692	0.211190	0.113824	0.063633
20	0.188317	0.186856	0.184539	0.112111	0.063539
25	0.167693	0.166853	0.165495	0.110057	0.063416

Table 4. Resultant shear stress τ_2 at the plate $\eta = -1$ for $G = 0.2$.

M^2/K^2	1.0	2.0	3.0	25.0	81.0
10	0.355559	0.347190	0.238894	0.165038	0.093297
15	0.295138	0.291708	0.505540	0.163032	0.093175
20	0.257682	0.255926	0.181505	0.160462	0.093105
25	0.231636	0.230604	0.163680	0.157465	0.092804

The primary and secondary velocity profiles have been plotted versus η for various values of K^2 and G (when flow does not separate) in Figs. 1 and 2. In Fig. 1 it is found that for fixed G , the primary velocity u decreases while the secondary flow is of an oscillatory nature with increase in K^2 . Figure 2 reveals that when K^2 is small, the primary velocity increases near the lower wall $\eta = -1$ while it decreases near the upper wall $\eta = 1$ with the increase in G . The effect of G on the secondary velocity ($-v$) is reversed as compared with the effect on the primary velocity u . It may be noted that due to the presence of buoyancy force, the velocity profiles are no longer symmetric.

The magnetic field components B_x and B_y have been depicted versus η for various values of K^2 and G in Figs. 3 and 4. It is observed from Fig. 3 that the magnetic field component B_x decreases with the increase in K^2 while the magnetic field component B_y is of oscillatory character with the increase in K^2 .

Figure 4 reveals that the magnetic field components B_x and B_y decrease with the increase in G .

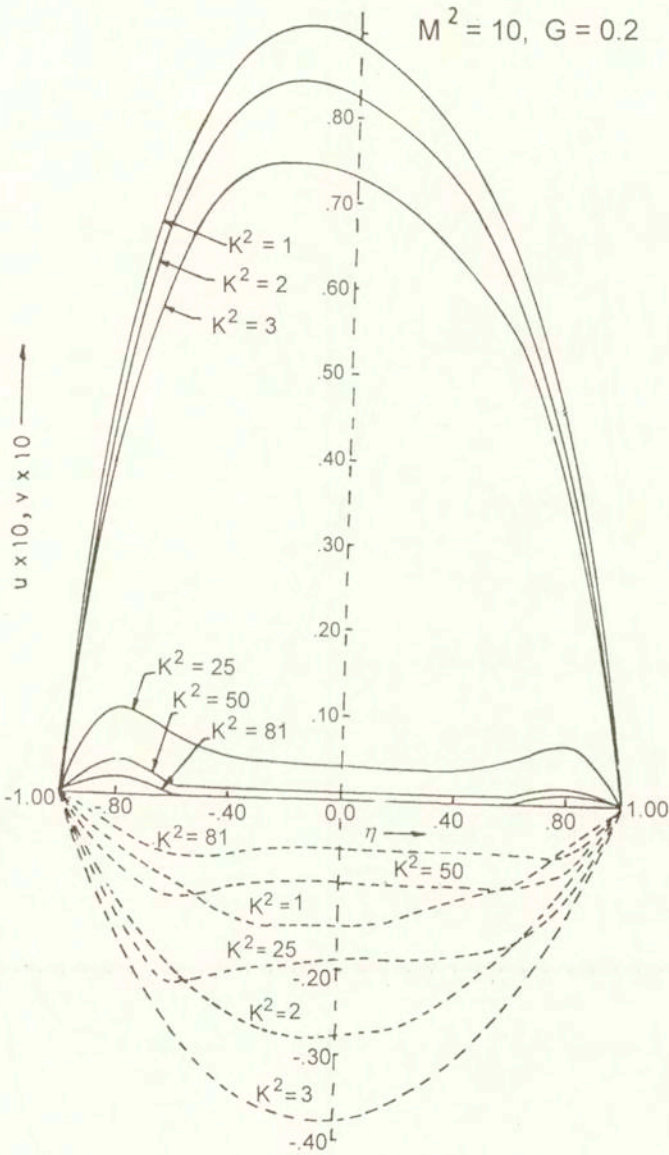


FIG. 1. Velocity distributions (— $u \times 10$, - - - $v \times 10$) in primary and secondary flow directions.

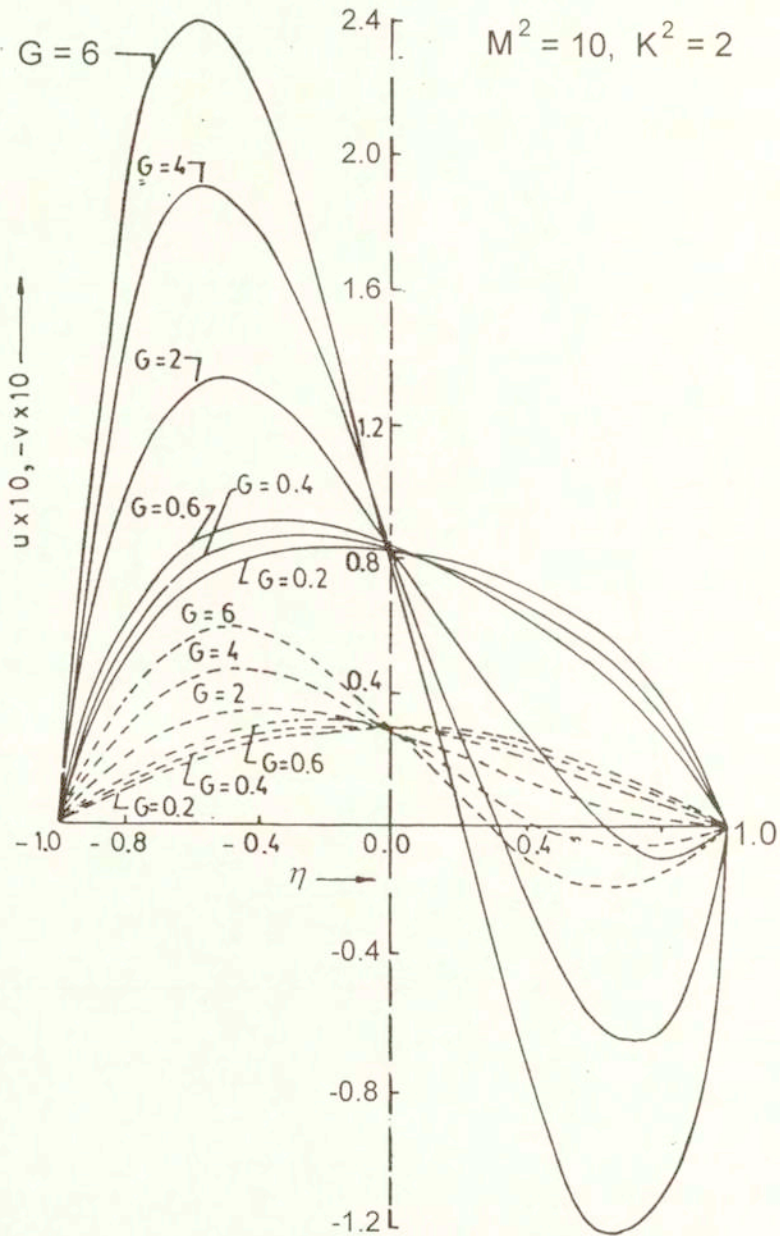


FIG. 2. Velocity distributions (— $u \times 10$, - - - $v \times 10$) in primary and secondary flow directions.

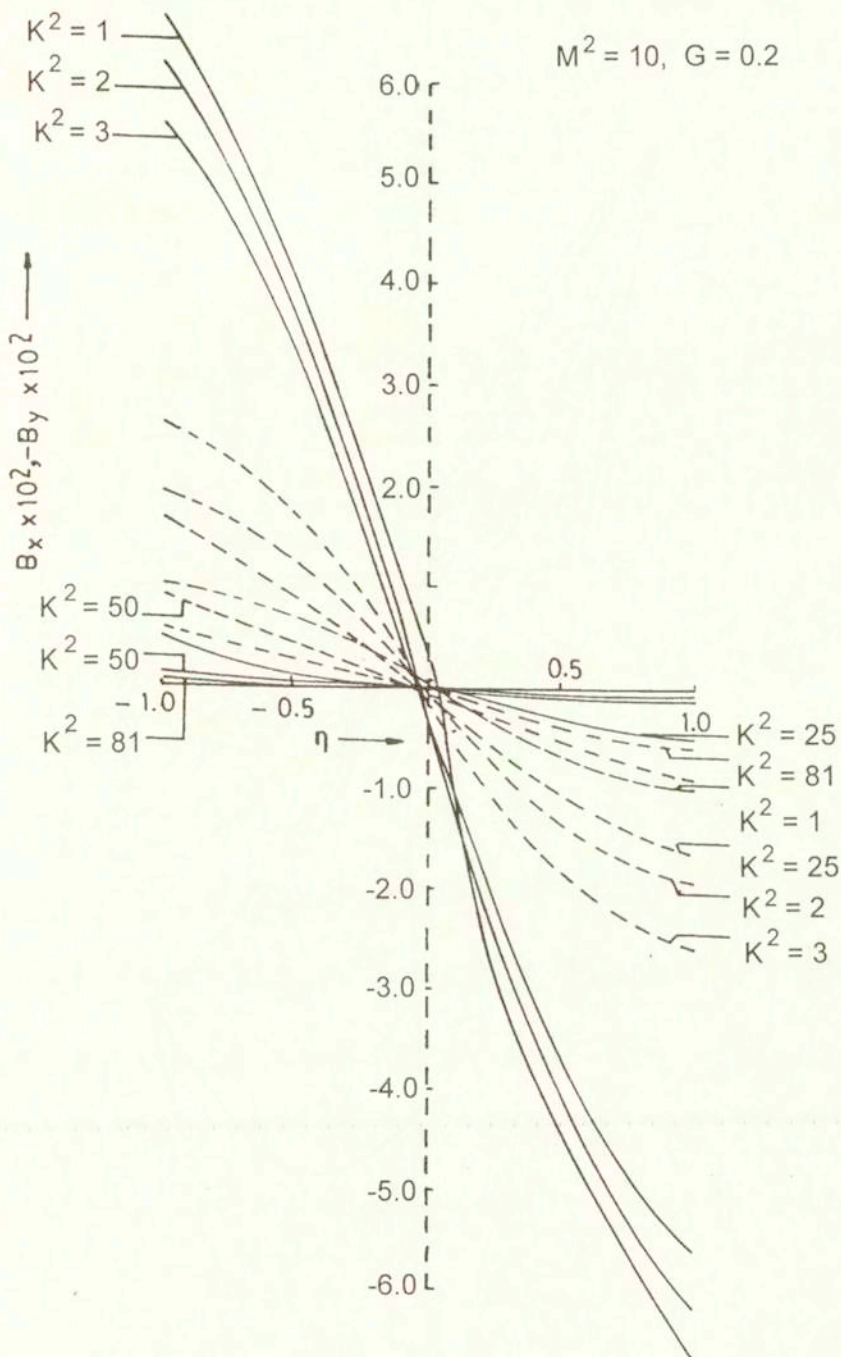


FIG. 3. Magnetic field distributions ($- B_x \times 10^2, - - - B_y \times 10^2$) in primary and secondary flow directions.

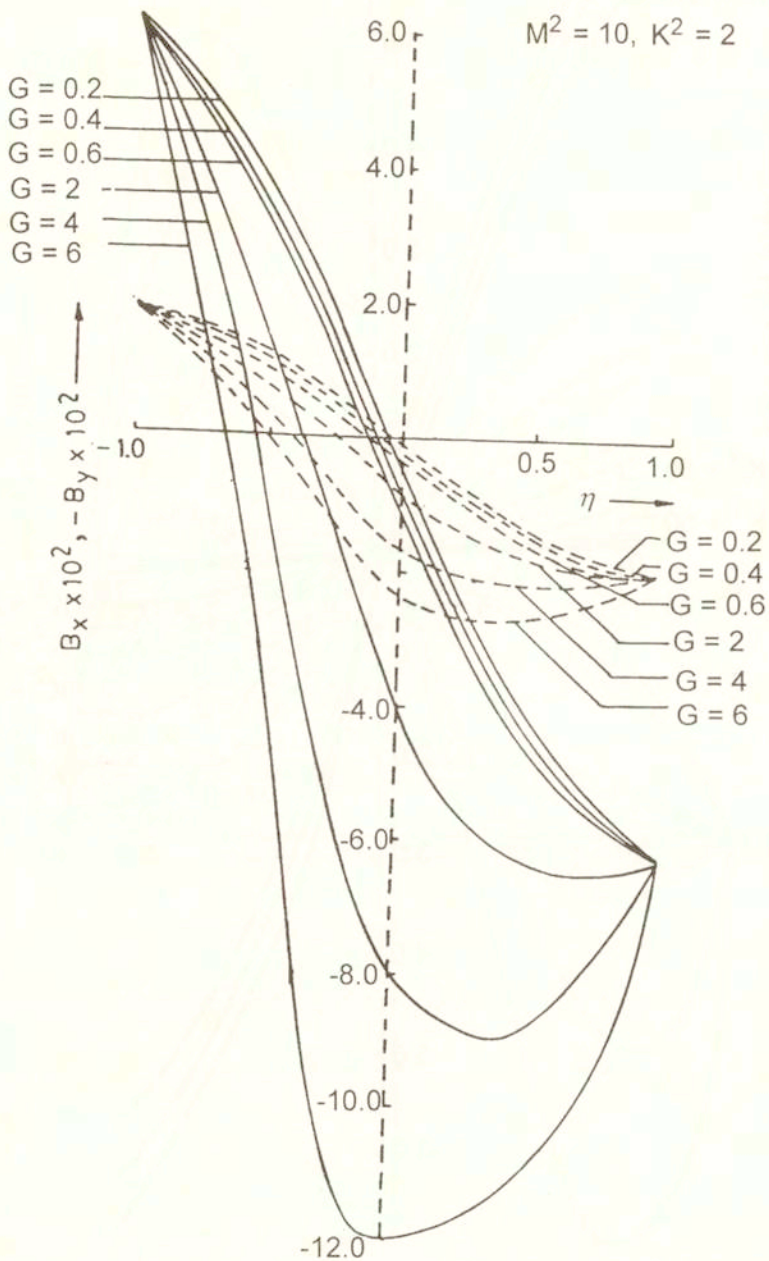


FIG. 4. Magnetic field distributions ($- B_x \times 10^2$, $- - - B_y \times 10^2$) in primary and secondary flow directions.

4. Heat transfer

For the fully developed flow, the energy equation is

$$(4.1) \quad u^* \frac{\partial(T - T_0)}{\partial x} = \frac{K}{\rho_0 C_p} \frac{\partial^2(T - T_0)}{\partial z^2} + \frac{\mu}{\rho_0 C_p} \left[\left(\frac{du^*}{dz} \right)^2 + \left(\frac{dv^*}{dz} \right)^2 \right] \\ + \frac{1}{\mu_e^2 \rho_0 \sigma C_p} \left[\left(\frac{dB_x^*}{dz} \right)^2 + \left(\frac{dB_y^*}{dz} \right)^2 \right],$$

where C_p is the specific heat at constant pressure and k is the thermal conductivity. The last two terms in the parentheses are the viscous and Joule dissipation, respectively.

Using (2.6), (2.7), (2.10) and (2.19), Eq. (4.1) becomes

$$(4.2) \quad \frac{d^2\theta}{d\eta^2} = P_r u - K_1 \left[\frac{dF}{d\eta} \frac{d\bar{F}}{d\eta} + M^2 \frac{db}{d\eta} \frac{d\bar{b}}{d\eta} \right],$$

where

$$P_r = (\mu/K)C_p, \quad \theta(\eta) = \phi/NL, \quad K_1 = \rho_0 \nu^2 R / KNL^3,$$

$$\frac{dF}{d\eta} \frac{d\bar{F}}{d\eta} = \left(\frac{du}{d\eta} \right)^2 + \left(\frac{dv}{d\eta} \right)^2, \quad \frac{db}{d\eta} \frac{d\bar{b}}{d\eta} = \left(\frac{dB_x}{d\eta} \right)^2 + \left(\frac{dB_y}{d\eta} \right)^2.$$

We assume the reference temperature T_0 in such a way that temperature at the plate $\eta = -1$ is $T_0 + Nx$ and thus, by virtue of (2.6), we get $\phi(-1) = 0$. Hence the temperature boundary conditions are

$$(4.3) \quad \theta(-1) = 0 \quad \text{and} \quad \theta(1) = \phi(1)/NL = N_1(\text{say}),$$

where N_1 is the wall temperature parameter.

Substituting the values of $F(\eta)$ and $b(\eta)$ from Eqs. (2.21) and (2.22) in Eq. (4.2) and solving the resulting differential equation subject to the boundary conditions (4.3), we obtain the expression for $\theta(\eta)$ which is rather complicated. We omit the details of calculations since they are lengthy. We have calculated numerically the rate of heat transfer at both the plates for various values of K^2 and G and presented the results in Tables 5 and 6. It is observed from Tables 5 and 6 that the rate of heat transfer at both the plates decreases with the increase in G . On the other hand, with increase in K^2 , the rate of heat transfer at the upper plate increases while that at the lower plate decreases.

Table 5. Rate of heat transfer $\left. \frac{d\theta}{d\eta} \right|_{\eta=1}$ for $P_r = 0.025$, $K_1 = 0.5$, $N_1 = 0.5$ and $M^2 = 10$.

G/K^2	1.0	2.0	3.0	25.0	81.0
0.0	0.218247	0.220370	0.223320	0.247559	0.249672
0.2	0.201979	0.204935	0.209022	0.244038	0.248510
0.4	0.185251	0.189052	0.194295	0.240429	0.247332

Table 6. Rate of heat transfer $\left. \frac{d\theta}{d\eta} \right|_{\eta=-1}$ for $P_r = 0.025$, $K_1 = 0.5$, $N_1 = 0.5$ and $M^2 = 10$.

G/K^2	1.0	2.0	3.0	25.0	81.0
0.0	0.134156	0.131785	0.128517	0.102536	0.100336
0.2	0.103589	0.102013	0.099832	0.084113	0.081915
0.4	0.073481	0.072689	0.071576	0.065779	0.068062

Acknowledgment

We are grateful to the referee for his helpful suggestion for the preparation of this paper. One of the authors (S.K. GHOSH) is sincerely acknowledged to University Grants Commission for financial support in persuing work under the scheme "Minor Research Project".

References

1. V. VIDYANIDHI, *Hydromagnetic flow in a channel with non-conducting walls*, J.Math. Phys. Sci., **3**, 193, 1969.
2. R. S. NANDA and H. K. MOHANTY, *Hydromagnetic flow in a rotating channel*, Appl. Sci. Res., **24**, 65, 1971.
3. P. S. GUPTA, *MHD combined free and forced convective flow in a rotating channel*, ZAMM, **54**, 359, 1974.

Received May 13, 1999; revised version January 10, 2000.